$$= \sum_{\mu=0}^{\infty} \frac{\beta_0^{\mu}}{\mu!} T_{\mu+m}(\beta) . \quad \text{(A5)}$$

In particular if β_0 is set equal to $-\beta$, we obtain a duplication formula

$$T_{\mu}(2\beta) = \sum_{l=0}^{\infty} \frac{(-\beta)^l}{l!} T_{\mu+l}(\beta) , \quad \text{(A6)}$$

and if β_0 is set equal to β, we obtain a sum rule

$$\sum_{\mu=1}^{\infty} \frac{\beta^{\mu-1}}{(\mu-1)!} T_{\mu}(\beta) = 1 . \quad \text{(A7)}$$

---

[1]T. Holstein, Phys. Rev. 72, 1212 (1947).
[2]T. Holstein, Phys. Rev. 72, 1212 (1947), Eq. (2.3).
[3]T. Holstein, Phys. Rev. 72, 1212 (1947), Eq. (2.21).
[4]T. Holstein, Phys. Rev. 72, 1218 (1947).
[5]The eigenvalues seem to be well separated. For a typical case ($\kappa = 2.5$), reported in the sphere calculation, the second root was nearly double the value of the lowest. The situation becomes more favorable as the radius becomes larger.
[6]T. Holstein, Phys. Rev. 83, 1159 (1961).
[7]The details of the arithmetic manipulation are similar to the procedures used in the sphere, discussed in text.
[8]Loss of significant figures was encountered due to the near-linear dependence of the higher-order $N_i(\xi)$. It probably would be more desirable to have chosen the $N_i(\xi)$ to have been the Legendre polynomials of even order.
[9]T. Holstein, Phys. Rev. 72, 1212 (1947), Eq. (4.22).
[10]T. Holstein, Phys. Rev. 72, 1212 (1947), Eq. (3.2).
[11]N. S. K. Menon and A. W. Nolle, the following paper, Phys. Rev. B 4, 3890 (1971).

PHYSICAL REVIEW B VOLUME 4, NUMBER 11 1 DECEMBER 1971

Radiation Imprisonment and Magnetic Field Effects on Luminescence in Pink Ruby*

N. S. K. Menon and A. W. Nolle
Department of Physics, The University of Texas, Austin, Texas 78712
(Received 20 July 1971)

The theory of imprisoned radiation developed by Holstein and recently extended by Scherr is adapted to apply to the luminescence decay in a solid. In addition to including a correction for losses from the excited level, it is necessary to consider reflections at the sample surfaces. Reflections are calculated approximately for a slab. The single Gaussian absorption function used in the reabsorption theory in lieu of an actual absorption function for the imprisoned radiation has the same integrated absorption I as the actual function and has a height equal to $\sqrt{2}I$ times the integral of the square of the actual function. Calculations are described for the ruby R lines, including the case where the Zeeman components are separated in a magnetic field. Experimental measurements of decay times at 77 °K of the ruby R lines are presented for samples having a Cr^{+3} concentration of approximately 10^{19} cm^{-3} and thickness from 0.6 to 13 mm. Magnetic fields up to 20 kG are used. The various decay times, lying between 5 and 12 msec, are predicted within about 5% by the theory, with the help of the approximate absorption corrections and of Zeeman component intensities given by Sugano and Tanabe. The R_1 line is used for most comparisons. Intensity increases of up to 100% in the steady-state R-line emission in a 20-kG magnetic field are shown to be accounted for by approximate treatments related to the decay-time theory. No change of transition probabilities with magnetic field is indicated by the foregoing results. Further observations suggest that the channels leading from the excitation levels for both single ions and pairs are affected by magnetic field, however. These observations include changes in the relative intensities of various pair lines when the field is applied, and a field-dependent difference in the emission intensities produced with blue and green excitation. Field-induced changes in pumping light absorption, if present, are insufficient to account for these variations.

I. INTRODUCTION

The theory of reabsorption of resonance radiation, also known as imprisonment, has been extensively treated by Holstein.[1] He provided working formulas for the limiting case of nearly complete reabsorption, which is important for gases. The calculations are troublesome for the case of a species having small peak absorption or present at small concentration (cases often encountered with solids), with the result that empirical approximations have been proposed[2] in lieu of the theory. Recently Scherr[3] has put the Holstein transmission function for a Gaussian line into a form convenient for partial reabsorption. From this he has evaluated the decay-time function for an infinite slab and also has extended the theory and the calculations to the case of a sphere.

We shall show that where sufficient information is available as to line shape and absorption cross

sections for resonance radiation, the theoretical results for a Gaussian line can be related to a system having more complicated line shape. This involves space averaging the cross section, for it is assumed in the theory that anisotropy of absorption is averaged out in the reabsorption process.

Varsanyi, Wood, and Schawlow[4] first demonstrated effects due to reabsorption in a solid, in connection with the luminescence decay time for the sharp red lines (R lines) due to Cr^{+3} in Al_2O_3 (ruby). The literature on ruby is now very extensive, and contains the necessary information to relate the behavior of the R lines quantitatively to the reabsorption theory, even in the presence of a magnetic field. We shall present luminescence decay-time measurements for several specimens of ruby differing as to the extent of reabsorption, and show that the theory is in reasonable agreement with these results when an approximate correction is made for reflections at the surfaces of the specimen. Then we shall show that the theory gives a good prediction of the decrease in decay time observed when the line components are separated in a magnetic field, and that the accompanying increase in emission under steady pumping can be related to the decay-time theory in suitable limiting cases. Radiation not significantly reabsorbed, such as vibronic emission, is a measure of the average density of excited species. Finally, with this understanding of reabsorption, we show that our results for ruby at 77 °K contain magnetic field effects not explainable by changes in reabsorption. These have to do with the excitation of both single-ion levels and pair levels by pumping.

II. THEORY

Holstein[1] has shown that imprisoned radiation phenomena depend on the transmission function $T_k(\rho)$, the probability that a resonant photon survives through distance ρ without reabsorption. For a Gaussian line with absorption coefficient k at the center, the function can be expressed as[3]

$$T_k(\rho) = \sum_{n=0}^{\infty} \frac{(-k\rho)^n}{n!(n+1)^{1/2}} \quad . \tag{1}$$

Variational solution of an integral equation involving $\partial T_k(\rho)/\partial\rho$ yields decay rates in the presence of reabsorption as eigenvalues, as well as approximate eigenfunctions (spatial distributions of density of excited atoms). For a sample of characteristic dimension L, containing excited atoms having radiative transition probability γ for the resonance (ground-state) transition that also causes reabsorption, let $\gamma F(kL)$ denote the decay rate of the slowest mode, as found by such a calculation. It will be shown that this result can be related to the present experiments by adding the decay-rate contribution for an additional mechanism not connected with reabsorption, and an approximate correction for reflection at the surfaces.

A. Effect of Losses from the Excited Level

Let there be another deexcitation mechanism of transition probability δ, so that the loss rate of quanta per unit volume is $(\delta+\gamma)n(\vec{r})$, where $n(\vec{r})$ is the density of the excited species. The rate of change of $n(\vec{r})$ at a point is

$$\frac{\partial n(\vec{r})}{\partial t} = -(\gamma+\delta)\, n(\vec{r}) + \gamma \int n(\vec{r}')G(\vec{r}', \vec{r})\, d\vec{r}', \tag{2}$$

which reduces to Holstein's (3.4) for $\delta = 0$. Here $G(\vec{r}', \vec{r})$ is a function pertaining to the transfer of quanta by emission and reabsorption, ordinarily taken to have the isotropic form $G(\rho) = -(1/4\pi\rho_2) \times \partial T_k(\rho)/\partial\rho$, where ρ is $|\vec{r} - \vec{r}'|$. Following through Holstein's solution with (2) as a starting point, one easily finds that δ is merely added to the result for decay rate; that is, the decay rate for the sample with reabsorption and also with the additional loss rate is

$$\tau^{-1} = \delta + \gamma F(kL) \ , \tag{3}$$

where $F(kL)$ [the right-hand member of Holstein's (3.10)] is the same eigenvalue in the variational problem as in the case $\delta = 0$, and the corresponding eigenfunction $n(\vec{r})$ is still correct. [Note: An experimental difficulty is accentuated when δ is the major contribution to τ^{-1}. When the actual initial distribution of excitation $n(\vec{r})$ in a luminescence decay experiment is quite different from the lowest eigenfunction for which (2) has an exponential solution, the decay rate corresponding to that eigenfunction is not immediately observed. Sufficiently large δ causes the radiation to become undetectably small before the decay becomes essentially $e^{-t/\tau}$.]

B. Approximate Correction for Reflection

This correction will be considered only for an infinite slab, bounded by the planes $z = \pm L/2$. In addition to the transfer function $G(\rho)$, we must include for first reflections the integral over the surfaces of $R(\theta_i)G(\rho_1)$, where ρ_1 is the path length from $\vec{r}_1$ to $\vec{r}_2$ via a single surface reflection, and $R(\theta_i)$ is the intensity reflection coefficient at the point of reflection, a function of the angle of incidence θ_i, suitably weighted for polarization directions $\vec{p}$. Multiple reflections, if significant, must be included similarly. A new and more difficult variational solution of the equation replacing (2) is required. We limit ourselves to the case where the reflection may be considered as a perturbation, with the old $n(z)$ retained. The parallel-slab problem has been solved[1, 3] by using a suitable integrated form of $T_k(\rho)$, denoted by $H(|z - z'|)$, which when multiplied by dz is the probability that a photon emitted at

z' is absorbed between the planes z and $z+dz$. For planes whose separation through a normal reflection path is ζ, let $H_r(\zeta)$ denote an analogous transfer function. This is given by $-\partial \mathcal{S}_r(\zeta)/\partial\zeta$, where

$$\mathcal{S}_r(\zeta) = \tfrac{1}{2}\int_0^{\pi/2} R(\theta_i)\, T(\zeta \sec\theta_i)\sin\theta_i\, d\theta_i . \qquad (4)$$

Transfer functions so defined for successive reflections should be added to Holstein's $H(\zeta)$ in the infinite-slab problem. In the present case, $R(\theta_i = 0)$ is small, only 0.036 for ruby in liquid nitrogen; more than 95% of the reflection correction arises from total internal reflection. Considering only this contribution, we have for the mth reflection

$$\mathcal{S}_r(\zeta) = \tfrac{1}{2}\int_{\theta_c}^{\pi/2} T(\zeta_m \sec\theta_i)\, \sin\theta_i\, d\theta_i , \qquad (5)$$

independent of polarization, where θ_c is the critical angle, 43°. Here ζ_m is the plane-to-plane normal distance by a path having m reflections. Using $H_r(\zeta_m) = -\partial \mathcal{S}_r(\zeta_m)/\partial\zeta_m$ in addition to the transfer function $H(\zeta)$ in Holstein's calculations we have

$$\frac{\tau^{-1}}{\gamma} = 1+\frac{\delta}{\gamma} - \frac{1}{Q}\iint n(z)\, n(z')\, H(|z-z'|)\, dz\, dz' - \frac{2}{Q}\sum_{m=1}^{M}\iint n(z)\, n(z')\, H_r(mL-z-z')\, dz\, dz' . \qquad (6)$$

The limits are $z = \pm L/2$. Q is the normalization factor $\int n^2(z)\, dz$. The final term is the reflection correction. Because of the symmetry of the problem, the factor 2 properly takes both surfaces into account. For $\delta = 0$ and $H_r = 0$, (6) is equivalent to Holstein's (4.4), for which numerical results are available.[3] The right-hand side is then the function $F(kL)$. The approximate reflection correction was evaluated for $kL \lesssim 2$ with functions $n(z)$ taken from a variational solution using three functions.[5]

The result of (1) for small kL approaches e^{ϕ}, where $\phi = -0.707kL + 0.0387(kL)^2 + 0.0029(kL)^3$.[5] We used $\phi \simeq -0.64kL$ to approximate $T_k(\rho)$ within 5% up to $kL = 2$. Then H_r is approximately $0.32k\, E_1(0.64kL/\cos\theta_c)$, where E_1 is the first-order exponential integral.[6] The last term in (6) is easily found by a coarse mesh integration for an appropriate total number of reflections M. Somewhat below $kL = 0.4$, the correction approaches the size of the original result $F(kL)$, so that the perturbation approach is not justified. Figure 1 shows the decay-time calculation from (6) for the ruby R_1 line for several values of M, with the values of δ and γ given in Sec. IV. Further details of the calculations are given in Appendix A.

For $kL > 2$, the reflection correction is mainly due to the first reflection, but for $kL < 0.5$, the correction converges slowly. It is important to consider the number of corrections to be counted for a slab that is actually a short cylinder of diameter D, as in our case. Let θ' be the angle of incidence such that the solid angle between θ_c and θ' is the same as that between θ' and $\pi/2$. Consider radiation originating at the center of the sample. If the angle of incidence $\theta_m = \tan^{-1}[(2m-1)\, D/L]$, above which the path with m reflections passes through the edge of the sample, is less than θ', the mth reflection will not be counted. According to this rough criterion, the number of reflections counted for our slab samples is from 1 to 4.

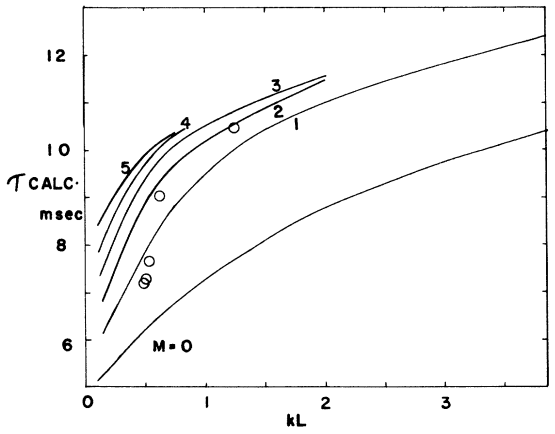

FIG. 1. Lower curve, τ given by (3) [same as (6) for $H_r = 0$], with $\delta = 65$ sec^{-1}, $\gamma = 148$ sec^{-1}, $F(kL)$ obtained as ϵ^{-1} from Ref. 3. Other curves calculated with (6) for several values of M, the number of reflections considered. Points give experimental τ for sample D, at $\theta = 60°$, for H from 0 to 16 kG. H has been converted to kL with the help of Fig. 4 (Voigt case). According to the criterion in the text, 1 to 1½ reflections should be considered for this sample.

C. Intensity of Luminescence under Steady Pumping

As shown in Sec. II D applying a magnetic field to the sample effectively reduces k. This causes a change in the observed intensity I of resonance radiation in which the following two competing effects are important: (a) When there is a constant creation rate P of excited states due to pumping, the increase of over-all loss rate τ^{-1} decreases the equilibrium population of excited states. In the limit $kL \ll 1$, only a small fraction of all quanta are affected by reabsorption in the steady state, and the effect may be neglected. In the limit of large kL the population varies as τ. (b) The increased transparency of the sample for the resonance radiation, expressed through the behavior of $T_k(\rho)$, allows more radiation to escape. These remarks are amplified in Appendix B.

A thorough treatment of these effects, requiring solution of (2) with a source function having the

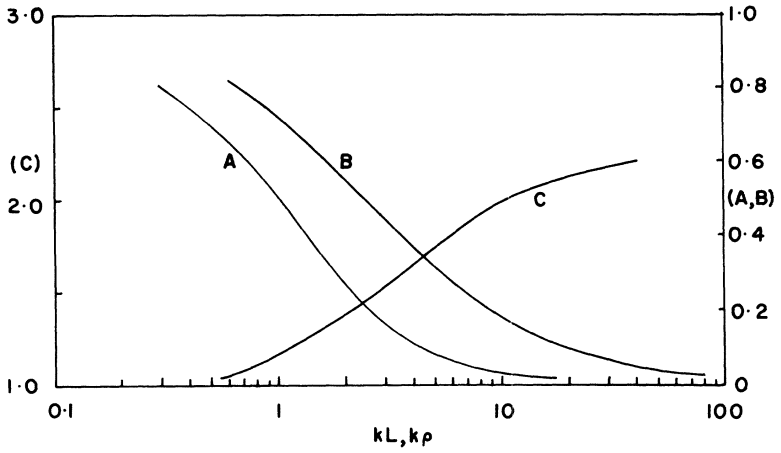

FIG. 2. A: Transmission function $T_k(\rho)$ from (1). B: Relative values of $(kL)^{-1}\int_0^L T_k(\rho)\,d\rho$, a measure of intensity from (7) when excitation is uniformly distributed. C: Factor by which the preceding function changes when kL is reduced to 40% of abcissa reading, applicable to ruby R_1 line when Zeeman components become resolved.

spatial distribution of the absorbed pump radiation and yielding a new excited-state distrubution $\mathfrak{N}(z)$, is beyond the scope of this paper. We shall only describe a limiting case that will be useful in considering the data. Let the sample lie within the range $z' = \pm L'/2$ along an optical path through the distant detector. Then the transmission function $T_k((L'/2) - z')$ gives the probability that radiation started toward the detector from a given depth penetrates to the sample surface $z' = L'/2$ facing the detector. Integrating this function with the excited-state distribution gives

$$I \propto \gamma P \int_{-L'/2}^{L'/2} \mathfrak{N}(z')\, T((L'/2) - z')\, dz'. \tag{7}$$

Figure 2 shows a normalized plot of (7), obtained with the transmission function (1), for $\mathfrak{N}(z') = \text{const}$. Below $kL' = 1$, nearly identical results would be obtained if $\mathfrak{N}(z')$ were a δ function at the center of the sample. Also plotted is $T_k(\rho)$, and a curve showing the factor by which (7) increases when a given value of kL' is reduced to 40%. It will be shown that this is approximately the effect of separating the Zeeman components of the ruby R_1 line.

D. Evaluation of k and its Magnetic Field Dependence

The parameter k must be such that the single Gaussian absorption function used in the reabsorption theory leads to the same $T_k(\rho)$ as does the actual absorption function. This correspondence is made for sufficiently small ρ as the following.

The absorption coefficient function in the actual sample is $If(\nu)$, where I is the integrated absorption coefficient and the infinite integral of $f(\nu)$ is unity. The $T_k(\rho)$ function is[1]

$$T_k(\rho) = \int_{-\infty}^{\infty} f(\nu)\, e^{-\rho I f(\nu)\, d\nu} \tag{8}$$

or approximately

$$T_k(\rho) \approx 1 - \rho I \int_{-\infty}^{\infty} f^2(\nu)\, d\nu\,. \tag{9}$$

We require the Gaussian absorption function, which has height k, also to yield integrated absorption I. Hence this function is $k \exp[-\pi k^2(\nu - \nu_0)^2/I^2]$. Upon finding $T_k(\rho)$ in the above manner from this function and equating the result to (9), we have

$$k = \sqrt{2}\, I \int_{-\infty}^{\infty} f^2(\nu)\, d\nu = \sqrt{2}\, N\sigma_T \left[\int \sigma^2(\nu)\, d\nu/\sigma_T^2 \right]\,. \tag{10}$$

The quantity in the square bracket is a property of the line shape for the system of interest.

Our specific application is to Cr^{+3} in Al_2O_3 (ruby). The resonance radiation of interest is the pair of sharp lines originating on the metastable ^2E level, which are found at approximately 6932 and 6919 Å at 77 °K and are known, respectively, as the R_1 and R_2 lines. Other mechanisms which deplete this level are vibronic radiation processes, transfer of quanta to ion pairs, and possible radiationless decay, which apparently causes only a very small fraction of the total rate of loss from ^2E. It does not seem necessary to summarize comprehensive discussions of the luminescence mechanisms available elsewhere[7-12]; sources will be cited as necessary for specific information. By numerical integration of the R_1 line shape in Fig. 4 of Ref. 7, we find the quantity in the square bracket in (10) to be 1.28. Taking total R_1-line cross sections as twice the values in cm^2 in Table II of Ref. 7, and using the weighting $\frac{2}{3}\sigma_\perp + \frac{1}{3}\sigma_\parallel$, we get

$$k = 3.7 \times 10^{-19} N\,, \tag{11}$$

where N is the Cr^{+3} population per cm^3, as the proper equivalent peak absorption coefficient at $H = 0$ for the Holstein theory.

Suppose the line-shape function can be expressed as $f(\nu) = \sum_1^p a_i f_i(\nu)$, where $\sum_1^p a_i = 1$, and $f_i(\nu)$ are well-known normalized functions. Calculations made in this way for overlapping components will be shown later. For the present consider the case where all $f_i(\nu)$ are the same shape function

$f_a(\nu - \nu_{0i})$ except that the center frequencies may differ, and where effects of overlap may be neglected. Then (10) gives

$$k = \sqrt{2}\ I[\int_{-\infty}^{\infty} f_a^2(\nu - \nu_{0i})\ d\nu]\sum_1^p a_i^2\ , \qquad (12)$$

which gives $T_k(\rho)$ correctly in the limit of small ρ. If the relative intensities a_i are equal, the proper value of k is p times the value that would be correct for one line having the average component intensity. [If the components are Gaussian, this conclusion is not limited to small ρ, but can be derived from (8).[1]] It is also easy to show that superimposed components can be combined into a single component having the aggregate intensity, before the preceding rule for combining nonoverlapping components is applied. These properties are contained in (12). For example, in zero magnetic field a ruby R line for a given Cr^{+3} isotope consists of two superpositions of components with centers separated by 0.38 cm^{-1}, whereas for $H \gtrsim 16$ kG the spectrum with H at 60° from the c axis consists of eight more or less resolved components. If all component amplitudes were equal, the ratio of effective k values for these two cases would be 4 : 1.

The quantity $k' = I\int f^2(\nu)\ d\nu$ might be called the thin-sample reabsorption coefficient, in view of (9). The ordinary absorption profile is squared here because it appears both in emission and in absorption (for zero Stokes shift). The discussion above shows that for a very thin sample, where L times the largest term in (12) is less than about 0.1, k is proportional to k', and that for even thick samples of ruby this function is an approximate measure of k for $H = 0$ and for $H \gtrsim 16$ kG. We have calculated k' for several values of H and for several angles. The function $f(\nu)$ used for a particular case is sketched in Fig. 3. The shapes used for the line components are described later. The amplitudes a_i were taken to be proportional to the total squared matrix elements of the Zeeman components, given for $\theta = 0°$ and 90° by Sugano and Tanabe.[8] The transformation to other angles is described by Sugano, Schawlow, and Varsanyi.[9] To relate the two proportionality constants π and σ in Ref. 7 pertaining to polarizations parallel and perpendicular to the c axis, we used $\sigma = 2\pi$, as suggested by experimental Zeeman spectra.[10] In view of the strong depolarizating effect of reabsorption,[1] we did not consider different polarizations separately. The center frequencies of the Zeeman components of R_1 and R_2 were found by use of the anisotropic g values for the excited states[11] and of matrix calculations[12] for the ground states. The low-field mixing of states[12] was not taken into account, however; high-field descriptions of the matrix elements were used throughout. Amplitudes of the components are given in Appendix C.

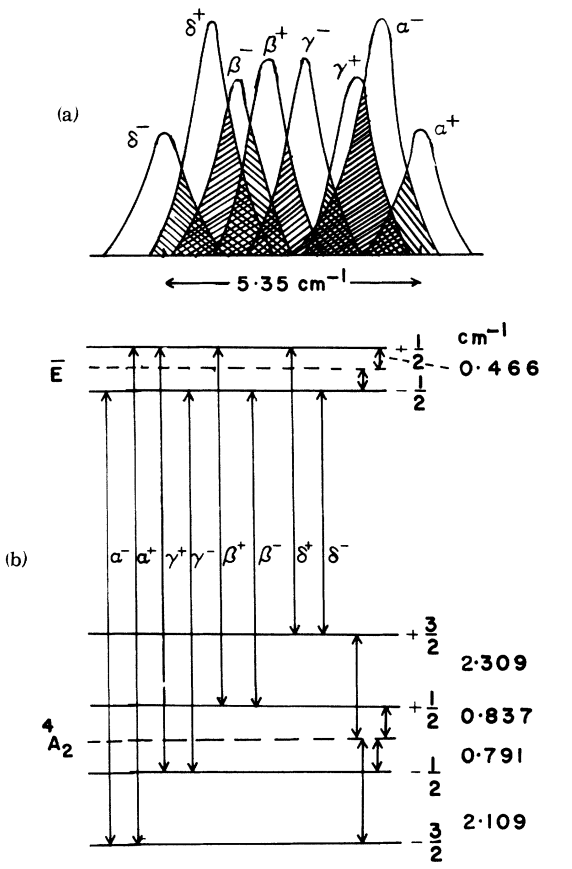

FIG. 3. (a) Sketch of R_1 Zeeman components in terms of a single shape function $f_a(\nu - \nu_{0i})$ repeated at center frequencies ν_{0i} with amplitudes a_i. For a thin sample the absorption coefficient k in the Holstein theory is proportional to the integral of $[\sum a_i f_a(\nu - \nu_{0i})]^2$, which decreases with reduction in overlap of the components. Shown for $\theta = 60°$, $H = 16$ kG. (b) Component notation, from Ref. 8, with +, − added to shown origin on upper or lower level of Kramers doublet.

Some results of the preceding calculations are shown in Fig. 4. In one set of calculations, the line component shape function $f_a(\nu)$ is a Voigt profile[13] having a full Gaussian width contribution of 0.108 cm^{-1} and a full Lorentz contribution of 0.065 cm^{-1}, essentially the values determined by Nelson and Sturge[7] for the R_1-line components at 77 °K. These values become $a = 0.5$ and $w = 0.0735$ cm^{-1} in terms of Ref. 13. Additional results are shown for a Gaussian profile of full width 0.32 cm^{-1} at half-power. The ratio $k'(H = 0)/k'(H \to \infty)$ for a given θ is only slightly different for these two functions. The small difference that does exist is due to a slight difference in the overlap at $H = 0$. Only a single isotope was considered in the calculations. The effect of natural isotopic abundances on the R-line spectra is known.[14] The extreme case that we have considered, the 0.32-cm^{-1} Gaussian, rep-

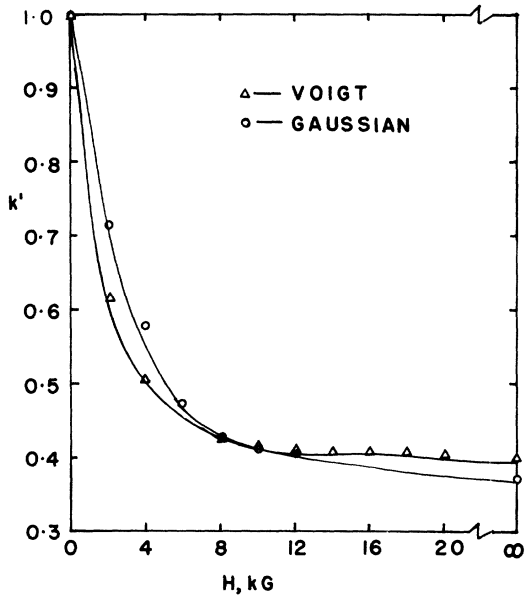

FIG. 4. Relative value of the effective absorption coefficient k (or of k') as a function of H, to be used in applying Holstein theory to a thin sample. Calculations done as described under Fig. 3 for R_1 line, 60°. Absolute values at zero field are given by (10) or (11). Results shown for both Voigt and Gaussian profiles, as described in the text, used for $f_a(\nu - \nu_{0i})$.

resents more broadening than is actually contributed by isotope effects.

III. EXPERIMENTAL WORK

The ruby samples were sawed from a roughly hexagonal flux-grown boule and polished to the final dimensions reported in Sec. IV. The longest sample (E) was polished on three adjacent side faces as well as on the cut ends. It was verified by x-ray diffraction that the c axis was along the axis of the boule within 10°. Concentrations were determined by comparing the absorption spectra with those published by Dodd *et al.*[15]

Figure 5 shows the experimental arrangement for intensity measurements. A lens system of aperture $f/4$ produces a spot of exciting light approximately covering the sample. The 0.5-m monochromator, aperture $f/6$, is provided with 0.6-mm slits. With this choice the R_1 and R_2 lines are adequately resolved, while the intensity corrections for Zeeman shifting of line components toward the shoulders of the response curve are only a few percent at maximum field. An XY recorder with a Hall probe, indicating the amplified dc output of the photomultiplier, was useful in initial surveys. The data to be shown were more accurately obtained by setting the field at various fixed values and integrating the dc signal, either with a circuit having an 18-sec time constant, or with a counter which samples a digitally converted form of the signal several hundred times during an interval of 10 sec. For decay-time measurements, the exciting light is chopped periodically, and the decay function is accumulated in a signal-enhancing multichannel analyzer, with appropriate background subtraction.

The sample is suspended in liquid N_2 in a transparent Dewar, with the c axis in the horizontal plane. Adjustment of the angle θ between the c axis and the magnetic field is made by rotating the sample holder about a vertical axis. The light source and the monochromator are on opposite sides of the magnet gap, in the same horizontal plane as the sample. The optical paths are perpendicular to the field.

Initially a different experimental setup was used, with the emitted light passing through a hole in the magnet pole cap and the sample in an optical Dewar with flat windows. Both linear and circular polarizers, as well as depolarizing films, were used in the detection path in a number of intensity studies. The differences associated with polarization were small in comparison to the intensity changes with magnetic field which we present in this paper, obtained without polarizers.

IV. RESULTS AND INTERPRETATION

The various ruby samples used in our study at 77 °K are described in Table I. The evaluations of k and of the number of reflection corrections to be counted have already been described; the entry "$1\frac{1}{2}$" indicates that the criterion for discarding the second reflection is marginally realized, so that it is appropriate to average the results for one and two reflections.

An initial decision as to whether to lump together the R_1 and R_2 transitions is required. In all of our measurements, these lines differed in decay time, in intensity variation with magnetic field, and in

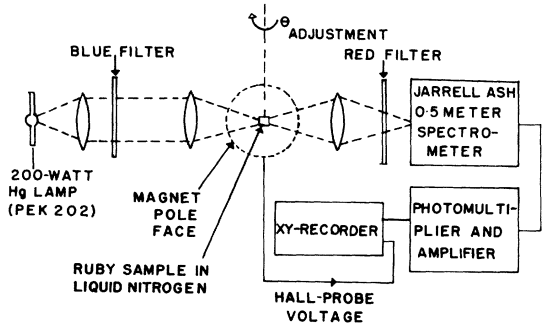

FIG. 5. Experimental arrangement for intensity measurement. In decay-time measurements the source light is chopped and a signal-enhancing multichannel analyzer receives the photomultiplier signal.

TABLE I. List of samples. Each is a slice, with polished faces, from a roughly hexagonal boule, diameter of inscribed circle approximately 1.3 cm. Thickness dimension is along c axis.

Designation	Thickness (cm)	Concentration (10^{19} cm^{-3})	No. of reflections considered	kL ($H=0$)
A (powder)	≈0.00	1.0	···	
B	0.059	0.9	4	0.19
C	0.165	0.9	$1\frac{1}{2}$	0.56
D	0.239	1.4	1	1.25
E	1.32	1.54	···	5.1[a]
F[b]	1.32	1.54	Large	7.4

[a]Value of kR for equivalent sphere; R chosen to match surface area of E.

[b]Same as E, but with sides and 70% of ends reflectively coated.

the angular dependence of the magnetic effects. Therefore thermalization of the levels involved in these transitions is incomplete. A formally correct treatment involving coupled differential equations would unduly complicate the application of the reabsorption theory. Accordingly the discussion will refer mainly to the R_1 line, and the constants to be used in calculations will be chosen to describe the decay time of that line correctly in the limit of zero reabsorption. In the present experiments, the R_1 line is the more important in energy balance, having an intensity almost exactly twice that of R_2.

A. Determination of Rate Constants

The powdered sample (A) has negligible reabsorption. The decay times observed with it from 0 to 20 kG are 4.70 ± 0.07 msec for R_1 and 4.31 ± 0.2 msec for R_2, with no systematic variation with H within these limits. The average of these results agrees with a composite R_1 and R_2 decay measurement by Nelson and Sturge.[7] Our result for R_1 gives $\gamma + \delta = 213 \pm 3$ sec^{-1}, independent of H, for use in further calculations. We shall treat γ and δ as individually independent of H. One justification is found in the work of Boiko *et al.*,[16] who concluded that the integrated R-line absorption coefficient in a sample similar to ours, at room temperature, is constant within an experimental error of 5 to 7% up to 100 kG. In the present work, if we assume that the vibronic radiation is a measure of the loss rate δ, we conclude that this quantity is effectively constant. Between 0 and 20 kG there is no change in the amplitude of the 7140-Å vibronic peak that cannot be explained by keeping δ constant within about 5%.

The coated sample F has a very large reabsorption, and therefore has $\tau^{-1} \approx \delta$. Observation of the decay time by means of R_1 line gave a highly accurate exponential decay (down to less than 20% of initial intensity) with time constant 16.6 msec. By trying various positions for windows in the reflective coating on a cylinder of length 3 cm, we produced decays both faster and slower than this one, with some departures from exponential behavior. This is apparently the situation described in Sec. III, where the signal becomes unobservably small before a pure decay eigenmode is reached. It was found, however, that all pair lines studied with sample F (7009, 7041, 7058, and 7119 Å) had accurately exponential decays, as expected if these lines monitor the total number of Cr^{+3} ions in the ^2E levels. At $H=0$ these decay curves have $\tau = 15.4 \pm 0.2$ msec, in agreement with the result obtained by Nelson and Sturge[7] from a suitable exponential portion of the decay of $R_1 + R_2$ radiation from a very long reflectively coated sample. This result gives $\delta = 65$ sec^{-1} (not a property of the R_1 or R_2 transitions, since this rate represents other losses from ^2E), completing the determination of constants used in calculating the theoretical decay time curves in Fig. 1.

B. Decay Time

Measured decay times for various values of H are shown in Fig. 6, which is for $\theta = 60°$. Additional measurements for other angles are shown in Fig. 7

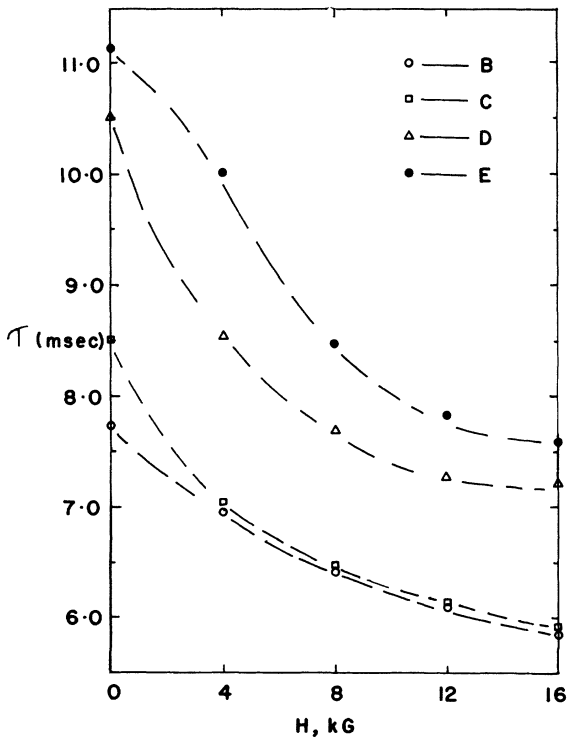

FIG. 6. Decay time of R_1 emission for several values of magnetic field strength at 77 °K, $\theta = 60°$. Sample thickness increases in the order B, C, D, E, as shown in Table I.

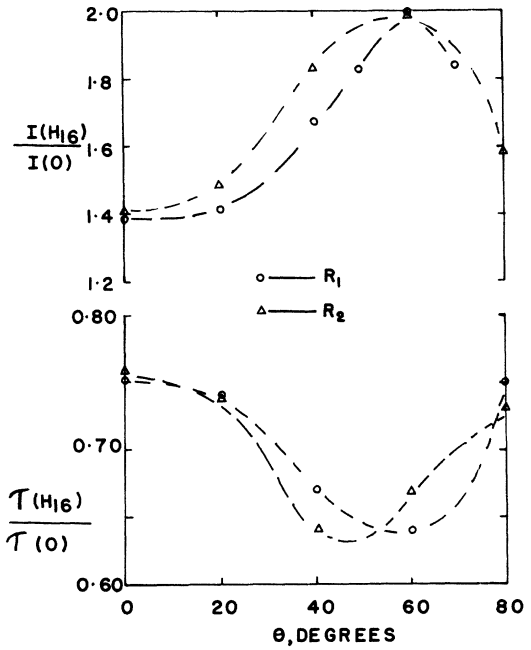

FIG. 7. Summary of angular variation and of difference between results for R_1 and R_2 lines. Top: Ratio of intensity at 16 kG to that in zero field as a function of θ, for both R_1 and R_2. Sample E (1.3 cm), 77 °K. Bottom: The corresponding ratio of decay times.

as a plot of high-field decay time divided by zero-field decay time, as a function of θ. A comparison of measured and calculated decay times is given in Table II. For slab samples, the calculated times at $H=0$ were found from Fig. 1 with the data given in Table I; for the high-field case, each kL is multiplied by 0.4. For the sample treated as a sphere (E), the starting point is the appropriate table of results given by Scherr.[3] The average disagreement of 5% in Table II seems satisfactory in view of the use of approximate perturbation corrections for reflection, although the error is not random; the observed low-field-to-high-field decay-time ratio is always greater than that calculated. A further comparison is given by the points in Fig. 1, showing observed decay times for sample D in relation to calculated curves. Because this is a relatively thin sample, the variation of k with H was considered to be the same as that of the thin-sample reabsorption coefficient in Fig. 3.

C. Intensity

Measurable increases in the intensity of the R lines with increasing magnetic field were found with all samples except those with extremely small absorption, A and B. Representative data are shown in Fig. 8, where θ is constant but H is varied, and in Fig. 9, where the high-field-low-field intensity ratios for the R_1 and R_2 lines are shown as a function of θ for sample E.

As pointed out in Sec. II, it is expected that the behavior of the intensity for thin samples can be found approximately by considering only mechanism (b), the effect of magnetic field on the transmission function, through Eq. (7). A comparison of values of the high-field-low-field intensity ratio from (7) with experimental results is shown in Table III. The high-field intensites for thin samples B, C, D are somewhat overestimated by this method. The fairly good prediction from (7) for sample E is perhaps fortuituous, because change of total population [mechanism (a)] is expected to be important for $kL>>1$. For this sample, however, the intensity results are well explained by referring to the idealized situation where the relation between total excited population and radiated power is the same as in free decay, so that changes of intensity can be calculated from changes in τ (see Appendix B). This approximation also predicts correctly the behavior of intensity of intermediate values of H, as shown for the R_1 line in Fig. 8 for sample E, and explains the angular variation of the intensity effect and the differences between the R_1- and R_2-line intensity changes (Fig. 7) in terms of corresponding variations observed in τ. The approach relating intensity to τ is inapplicable when reabsorption is relatively small, as shown in Appendix B; Eq. (B1) greatly overestimates the intensity changes for samples B, C, and D.

Also shown in Fig. 8 is the effect of magnetic field on the intensity of two lines due to ion pairs. These were studied only with thick samples E and F, because of signal strength requirements. The behavior of the 7009-Å line differs significantly from that of the others observed. This is more fully considered below. Otherwise the intensities of the pair lines and of the 7140-Å vibronic peak behave in the same manner as the decay time, if we assign an experimental uncertainty of about 3% of each intensity curve. This is the expected result for a thick sample, where the excited-state population in a steady-state emission experiment is propor-

TABLE II. Calculated and measured decay times.

Sample (cm)	$H=0$ τ_{calc} (msec)	$H=0$ τ_{obs} (msec)	$H=18$ kG; $\theta=60°$ τ_{calc} (msec)	$H=18$ kG; $\theta=60°$ τ_{obs} (msec)
B (0.059)	8.4	7.8	a	5.8
C (0.16)	8.6	8.5	a	5.9
D (0.24)	10.0	10.3	7.9	7.2
E (1.3)	10.7–11.8[b]	11.1	7.9–8.5[b]	7.6

[a]Perturbation approach inapplicable.

[b]Spherical theory used; reflection correction unavailable. Results shown for no correction, and for correction making same contribution to τ^{-1} as first reflection in slab having $kL \approx 5$.

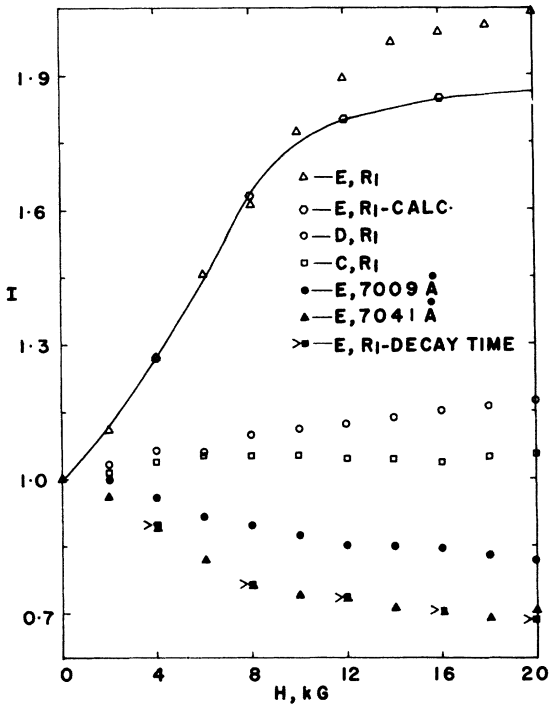

FIG. 8. Upper portion: Ratio of observed R_1 intensity to that at zero field for samples C, D, E, of successively greater thickness. The curve for sample E is calculated from experimental values of τ with (B1). Lower portion: Ratio of intensity to that at zero field for pair lines at 7009 and at 7041 Å, sample E, and also ratio of decay time to that at zero field, almost indistinguishable from 7041-Å intensity points. All data shown are for 77 °K, $\theta = 60°$.

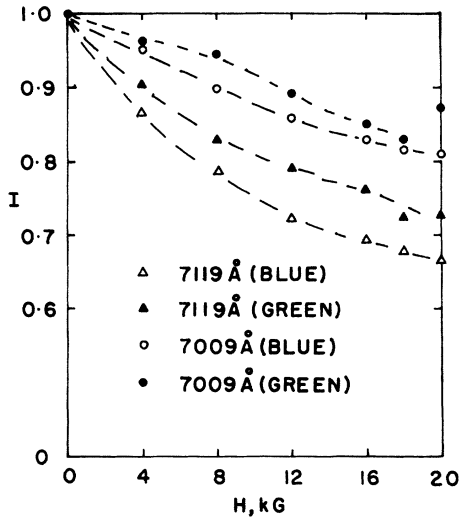

FIG. 9. Differential effect of magnetic field on 7009- and 7119-Å pair lines, and in experiments using blue or green excitation. Sample E (1.3 cm), 77 °K, $\theta = 60°$. Ratio of intensity to corresponding value in zero field is plotted in each case.

tional to τ as found in free decay, and where the effects of H on nonresonant radiation occur mainly through this population change.

Reabsorption effects at room temperature are very small with the ruby samples chosen for the present experiments. The total intensity increase for sample E is about 1% for the R_1 line and 2% for R_2—effects of the order of experimental error. The expected result at room temperature can be predicted approximately from data given by Boiko *et al.* Taking the absorption peak as a rough guide, we find that k for 300 ° K is of the order of 5% of the value for 77 °K, and that at 300 °K a field of 20 kG reduces k to about 0.9 of the original value. The calculated intensity increase for R_1 at 20 kG is of the order of 2%.

Over-all, it appears that with the approximations used here the intensity changes with magnetic field are understandable in terms of reabsorption theory, even though we have not attempted a complete solution for steady-state emission.

D. Effects of Angle; Comparison of R_1 and R_2

The emphasis in this paper has been on the variation of reabsorption phenomena with sample thickness and with Zeeman splitting. Therefore the discussions have mainly concerned the case $\theta = 60°$, where the initial variation of k with H is particularly large, and have been mainly for R_1 line. A few additional calculations for other angles and for the R_2 line as well as R_1 have been made with component amplitudes in Appendix C, all for only a single isotope. The reduction of k for completely resolved Zeeman components is the same within about 10% for R_1 and R_2, and is not strongly dependent on angle. The reduction of k for intermediate fields, 2–8 kG, is quite sensitive to angle, and in the neighborhood of 60 °–80 ° is greater for R_2 than for R_1. These predictions are borne out at least qualitatively in the experimental data. However, as shown in Fig. 7, these effects are found even at 16 kG, above the range where substantial variation of k is predicted. The angular effects should be further investigated, to determine whether consideration of isotopic abundances and possibly of polarization will explain the existence of angular variations at 16 kG and higher.

TABLE III. (Intensity at 16 kG)/(zero-field intensity) $\theta = 60°$, R_1 line.

Sample	Observed (±3%)	Calculated [Eq. (7)] transmission	Calculated from observed τ by (B1)
B	0.99	1.05	Inapplicable
C	1.05	1.12	Inapplicable
D	1.17	1.25	Inapplicable
E	2.00	1.92	1.85 (see Fig. 8)

E. Variation of Excitation with Magnetic Field

The magnetic field effects described above arise from the effect of the Zeeman splitting on reabsorption, and appear not to involve variations of transition rates with magnetic field. We shall now list other observations, which appear to show field-dependent effects in the excitation of single ions and pairs, and which warrant further investigation.

(i) In steady emission, the 7009-Å pair line (N_2), which is due to fourth nearest neighbors,[17,18] increases in intensity relative to the 7140-Å vibronic peak and to the other pair lines that we studied (7119, 7058, and 7041Å, due to second and third neighbors). The increase relative to the average of the 7119- and 7041-Å lines, shown in Fig. 8, is 22% at 20 kG. (Smaller differences occur between the intensity curves for other lines, but only slightly greater than the experimental uncertainty of 2–3%.)

(ii) This effect is not found in free decay. Using the coated sample (F), we obtained decay curves for all pair lines listed in (i), and used least-squares-fitted exponentials to compare amplitudes as well as decay times. Within a total variation of some 5% the amplitudes and the decay times for all these exponentials decreased together in the magnetic field, following the curve shown in Fig. 8 for the 7119-Å line in sample E. Therefore the magnetic field has no effect on transfer of quanta from the reservoir of excited ions in the ^2E that is sufficient to explain the behavior of the N_2 line in (i).

(iii) It appears to be well established that transfer of quanta from single ions to pairs occurs almost entirely from the ^2E single-ion level, and not from the absorption bands.[19,20] Since (ii) shows that this kind of transfer is not sufficiently affected by magnetic field to explain the behavior of the 7009-Å line in steady emission, it appears that this behavior is not due to changes in transfer from single ions at any level, but involves the decay channels that start with absorption of a quantum of pump light by the pair.

(iv) Magnetic field effects in the excitation process are also found for the R lines. The behavior of the steady-state emission intensity with magnetic field that we explained approximately on the assumption of constant transition probabilities was obtained with blue excitation. With green excitation (near 5460 Å), the intensity increase at 20 kG is about 5% greater than that shown in Fig. 8 for sample E. This differential also appears for pair lines, as shown in Fig. 9. Taken together with item (iii), this observation indicates that excitation processes starting with the absorption level are field dependent not only for pairs but also, at least for green absorption, in the case of single ions.

(v) We have been unable to explain these results in terms of a change in absorption cross section for the pumping light. By setting the monochromator to receive excitation light, we found that the absorption coefficient in the pumping bands does not change as much as 3% up to 20 kG. This experiment was done for the blue band with a filter of width 30 Å, centered at 4360 Å, in front of the source, and for the green band with a similar filter at 5460 Å.

The effect of magnetic field on the channels originating in the absorption levels seems to merit further investigation with samples of differing concentrations, and at lower temperatures.

V. DISCUSSION

In this investigation we have explored the range of the reabsorption parameter kL in which the emission properties of ruby at 77 °K are most severely affected by changes in reabsorption. Out of a possible limiting ratio of decay times of 3.3 the experiments covered a range of about 2.3 (excluding reflectively coated samples). In this range the theory of reabsorption accounts for the decay times within a few percent in spite of the need for large reflection corrections, which were done here by an approximate method only.

In experiments involving resonance radiation, even with small and relatively dilute solid samples, reabsorption effects can be a serious source of error. As an example, consider a ruby sample 1 mm thick, concentration 10^{19} cm^{-3}, 8 mm diam, in gas at 77 °K. With two reflections considered, the decay time is approximately 8.2 msec for the R_1 line, rather than 4.7 msec as for a much thinner sample. As another example, consider a thermoluminescence experiment that produces emission from the ruby ^2E level. The sample is a 1-cm cube with 10^{19}-cm^{-3} concentration. If there were a mechanism causing such emission at 77 °K, the power radiated in the R lines would be reduced because of reabsorption to approximately half the value which would be obtained with the same sample finely divided and dispersed. For a mechanism causing emission near room temperature there would be no appreciable correction. That is, changes of reabsorption can be important in experiments with solids in which there are large temperature-induced changes in linewidth, as well as in experiments where Zeeman splitting occurs.

The reabsorption theory based on Holstein's treatment, as opposed to approximations which could be made by assuming an exponential transmission function, is necessary for kL greater than about 1.5 to 2.0, according to the requirements in a particular case. Another statement of this result is that the attenuation of radiation by reabsorption is not exponential for intensity reductions below approximately $1/e$.

ACKNOWLEDGMENTS

We acknowledge the generous assistance of Kenneth M. Valentine and Richard J. Tropp in various phases of this work, and especially the invaluable help provided by Professor Charles W. Scherr in making available the results of his analysis and calculations as they were completed.

APPENDIX A: FURTHER REMARKS ON THE REFLECTION CORRECTION FOR A SLAB

By reflection correction we mean the last term in (6), which has the form $-\sum_{m=1}^{M} C_m$. For calculations by the perturbation method one is justified in using approximations to the transmission function $T_k(\rho)$ and also to the distribution function $n(z)$; the decay rates in the Holstein theory as well as C_m are not sensitive to small changes in the distribution.

In numerical integration to obtain C_m, the approximate form of H_τ given following (6) is adequate if the largest value that occurs for the argument of the E_1 function is no greater than about 2.4. Where this approximation is allowable, little additional error results from using a mesh width of $L/2$ for the integration. The result can then be expressed in terms of $[n_{av}(z)]^2/[n^2(z)]_{av}$, which is found from Scherr's three-term variational function[5] to be nearly constant (0.486 to 0.500 for $0 \leq kL \leq 2.0$). This procedure gives the formula

$$C_m \approx 0.08\, kL\, E_1[(2m-1)Y] + 2E_1(2mY) + E_1[(2m+1)Y], \quad \text{(A1)}$$

where $Y = 0.32\, kL/\cos\theta_c$, a good working estimate of the correction. In our case (A1) agrees within 10% with a fine-mesh calculation for $kL = 2$; for $kL = 1$ the agreement is within 1%, an unimportant deviation for a finite slab in view of the arbitrariness in determining M.

For calculations outside the range of the E_1 approximation for the transmission function, the starting point is $T_k(\rho)$ as given by (1), which joins smoothly at $kL = 12.5$ to Holstein's asymptotic formula,[1]

$$T_k(\rho) \approx [\rho(\pi \ln k\rho)^{1/2}]^{-1}.$$

It is suggested that a Gaussian function, $e^{-\alpha(2z/L)^2}$, would be an adequate approximation for $n(z)$ in further calculations. When α is chosen to duplicate the ratio of the surface value of $n(z)$ to that for $z = 0$ as listed by Scherr,[3] this function agrees within some 3% with the three-term variational functions in the range we have explored.

APPENDIX B: FURTHER REMARKS ON INTENSITY

If the steady-state excitation were to maintain a distribution of excited species identical to the eigendistribution $n(z)$ having the longest free decay time τ, then τ^{-1} would be a measure of the total loss rate, $\delta\tau$ would be the fraction of the loss not due to resonance radiation, and the power output P_{rad} of resonance radiation would behave as

$$P_{rad} \propto P(1-\delta\tau). \quad \text{(B1)}$$

Also, the total excited-state population would be proportional to $P\tau$.

In practice, the absorption of pump quanta can be nearly uniform through the sample, for small pump-light absorption, or in the opposite limit can be concentrated at one surface; a peaked distribution similar to $n(z)$ is not usual. In the limiting case of small reabsorption ($kL \ll 1$) the steady-state distribution $\mathfrak{N}(z)$ is entirely determined by the absorption of pump light. Thus ordinarily it also is quite different from $n(z)$, and contains a large admixture of higher eigenfunctions having free decay times smaller than τ. Consequently, when kL is small the full effect of reabsorption in terms of decay time is not found in the behavior of intensity; (B1) badly overestimates the intensity variation with magnetic field for our thinnest samples because of this. The division of the intensity behavior into the two effects (a) and (b) in Sec. II is an arbitrary but convenient way of describing the situation.

For $kL \gg 1$, most escaping quanta from a sample pumped on the side opposite the observer have been reabsorbed repeatedly. In this case (our sample E) it is not surprising that the excited-state population measured by nonresonance radiation is found to vary as τ, and that (B1) gives a good estimate of the changes of intensity with magnetic

TABLE IV. The intensities of different Zeeman components of R_1 and R_2 lines.

θ	α^+ or δ^-	α^- or δ^+	β^+ or γ^-	β^- or γ^+
		R_1		
0°	0	0.27	0.18	0.05
20°	0.01	0.26	0.17	0.06
40°	0.05	0.21	0.15	0.09
60°	0.09	0.16	0.13	0.12
70°	0.10	0.14	0.13	0.13
80°	0.12	0.13	0.13	0.12
90°	0.12	0.12	0.13	0.13
		R_2		
0°	0	0.17	0.22	0.11
20°	0.01	0.16	0.20	0.13
40°	0.05	0.16	0.13	0.16
60°	0.11	0.15	0.12	0.12
70°	0.13	0.15	0.11	0.11
80°	0.15	0.13	0.11	0.11
90°	0.15	0.15	0.10	0.10

field on the basis of the decay-time behavior. Equation (B1) is convenient because it does not involve the geometry of the sample, but it is not rigorous for intensity, because the distribution of power between the front and back surfaces of the sample is dependent on kL and on the excitation distribution.

APPENDIX C: INTENSITIES OF ZEEMAN COMPONENTS

The variation of reabsorption effects with angle occurs largely through the amplitudes a_i in Table IV. The method of obtaining these values from Refs. 7 and 8 is outlined in the text and more fully described elsewhere.[21] The component notation is given in Fig. 3.

*Work supported in part by the National Science Foundation.

[1]T. Holstein, Phys. Rev. 72, 1212 (1947). $T(\rho)$ and k_0 in this reference are written as $T_k(\rho)$ and k, respectively, in the present paper.

[2]J. Heber, K. H. Hellwege, and U. Köbler, Helv. Phys. Acta 41, 879 (1968).

[3]Charles W. Scherr, preceding paper, Phys. Rev. B 4, 3885 (1971).

[4]F. Varsanyi, D. L. Wood, and A. L. Schawlow, Phys. Rev. Letters 3, 544 (1959).

[5]Charles W. Scherr (private communication).

[6]*Handbook of Mathematical Functions*, edited by M. Abramowitz and I. A. Stegun (U.S. GPO, Washington, D.C., 1964), Appl. Math. Ser. 55.

[7]D. F. Nelson and M. D. Sturge, Phys. Rev. 137, A1117 (1965).

[8]S. Sugano and Y. Tanabe, J. Phys. Soc. Japan 13, 880 (1958).

[9]S. Sugano, A. L. Schawlow, and F. Varsanyi, Phys. Rev. 120, 2045 (1960), see Sec. III.

[10]S. Sugano and I. Tsujikawa, J. Phys. Soc. Japan 13, 899 (1958).

[11]J. P. Van der Ziel and N. Bloembergen, Phys. Rev. 138, A1287 (1965).

[12]E. O. Schulz-Du Bois, Bell System Tech. J. 38, 271 (1959).

[13]D. W. Posener, Australian J. Phys. 12, 184 (1959).

[14]G. F. Imbusch, W. M. Yen, A. L. Schawlow, G. E. Devlin, and J. P. Remeika, Phys. Rev. 136, A481 (1964).

[15]D. M. Dodd, D. L. Wood, and R. L. Barns, Phys. Rev. 35, 1183 (1964).

[16]B. B. Boiko, V. V. Valyavko, N. I. Insarova, and N. S. Petrov, Zh. Priklad. Spektrosk. (USSR) 11, 933 (1969).

[17]P. Kisliuk, N. C. Chang, P. L. Scott, and M. H. L. Pryce, Phys. Rev. 184, 367 (1969).

[18]M. J. Berggren, G. F. Imbusch, and P. L. Scott, Phys. Rev. 188, 675 (1969).

[19]G. F. Imbusch, Phys. Rev. 153, 326 (1967).

[20]R. J. Birgeneau, J. Chem. Phys. 50, 4282 (1969).

[21]N. S. K. Menon, dissertation (The University of Texas at Austin, 1971) (unpublished). (Available from University Microfilm in Ann Arbor, Mich.)

PHYSICAL REVIEW B VOLUME 4, NUMBER 11 1 DECEMBER 1971

Theoretical Magnetic Form Factors of Co^{++} and Fe^{++} in Their Monoxides

A. Mahendra and D. C. Khan
Department of Physics, Indian Institute of Technology, Kanpur, India
(Received 2 June 1971)

The spherical magnetic form factors of Co^{++} in CoO and Fe^{++} in FeO are calculated, including the effect of unquenched orbital magnetic moment. Expansions relative to the "spin-only" case are found to be 11% for Co^{++} and 9% for Fe^{++}. For CoO this is a major step in the quantitative explanation of the 15–17% expansion of the experimental curve compared to the Freeman-Watson "spin-only" curve. For FeO no good experimental data are yet available for comparison.

I. INTRODUCTION

The spherical magnetic form factor of a transition-metal ion is a measure of the charge-density distribution of the unpaired electrons of the unfilled $3d$ shell, and as such is of great importance in the study of physical properties of these ions. Halpern and Johnson,[1] in their theory of scattering of neutrons by these ions, derived an expression for the magnetic form factor. Weiss and Freeman[2] calculated the effects of the nonspherical charge distribution of the $3d$ electrons in various crystalline fields and thus made it possible to isolate the spherically symmetric form factor. The assumption in both these cases has been that the orbital magnetic moment is completely quenched by the crystalline field, and its associated magnetic moment does not contribute to neutron scattering.

However, an examination of the g factors of the transition-metal ions in different salts shows that there may be sizable residual orbital moments present.[3] In Co^{++} and Fe^{++} this would be expected, since the orbital degeneracy of the ground state is not completely lifted by the cubic crystalline field.[4] In Ni^{++} the degeneracy is completely lifted, but the spin-orbit coupling causes the admixture of a higher